INTENSITY DISTRIBUTION OF DOUBLY SCATTERED POLARIZED LASER RADIATION IN THE FOCAL PLANE OF LIDAR RECEIVER

Vadim Griaznov [(1)], Igor Veselovskii [(1)], Paolo Di Girolamo [(2)], Michail Korenskii[(1)], Donato Summa[(2)]

[(1)]*Physics Instrumentation Center, Troitsk, Moscow Region, 142190, Russia, E-mail: griaznov@pic.troitsk.ru, iveselov@pic.troitsk.ru*
[(2)]*DIFA, Univ.degli Studi della Basilicata, Potenza, Italy, E-mail: digirolamo@unibas.it*

ABSTRACT

Depolarization lidars are widely used for the study of clouds and aerosols because of their ability to discriminate between spherical particles and particles of irregular shape. Depolarization of cloud backscatter can be caused also by the multiple scattering events. One of the ways to gain information about particle parameters in the presence of strong multiple scattering is the measurement of azimuthally dependent polarization patterns in the focal plane of receiver. In this paper we present an algorithm for the calculation of corresponding polarized patterns in the frame of double scattering approximation. The computations are performed for different parameters of scattering geometry, e.g. cloud base and sounding depth. Intensity distribution of depolarized component is of cross-shape and rotated at 45 dg with respect to laser polarization. The use of a properly oriented cross-shape mask in the receiver focal plane allows removing a significant portion of depolarized component produced by double scattering. To verify it experimentally, cloud depolarization measurements were performed with different orientations of cross-shape mask. Results obtained from measurements are in qualitative agreement with the model prediction.

1. INTRODUCTION

Important information about cloud parameters can be obtained by the analysis of their response to a polarized laser source. Depolarization lidars are widely used in the study of clouds because of their ability to discriminate between spherical particles and particles of irregular shape. Depolarization of cloud backscatter can also arise as a result of multiple scattering. It is known that multiply scattered cross-polarized lidar returns can present a cross shape pattern that was first observed by Pal et.al.[1] The pattern contains retrievable information on cloud parameters, e.g., optical depth and droplet size, as well as information concerning the number of contributing scattering orders[2]. The theoretical description of this phenomenon was done in Ref.3,4 in the frame of double scattering approximation. That model includes assumptions which make more complicated the comparison of model prediction with the results of lidar measurements:

- scattering from semi-infinite space is considered, while the lidar probes a thin layer within a cloud, thus results depend on scattering geometry e.g. cloud base and scattering depth;
- the scattered photons propagate parallel to initial ones, while in lidar we are interested to evaluate the dependence of scattered power on telescope field of view (FOV) θ;

In our paper we present the results of simulations performed in the frame of the double scattering model which takes into account the specific features of lidar sounding mentioned above.

.

2. MODEL DESCRIPTION

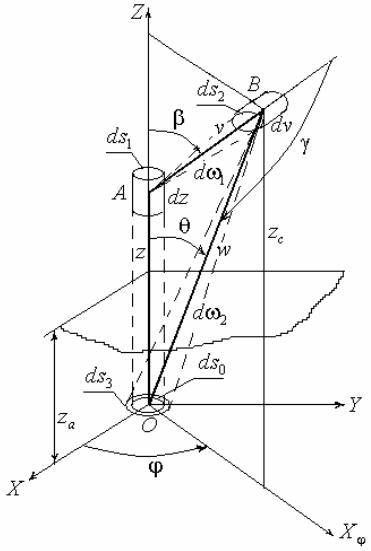

Fig.1. Geometry of scattering

The computations are performed for scattering geometry shown in Fig.1. The incident wave beam propagates parallel to the Z axis. The radiation is doubly scattered inside the cloud with base indicated by the plane at height z_a. First scattering occurs at the point A, and after second scattering at the point B the radiation returns to the lidar receiver at angle θ. The

lidar detects the scattered radiation from the distance R, i.e. the contribution of all scattering events for which total light path is $z+v+w=2R$ must be integrated. The laser beam divergence is assumed to be small, thus the single scattered radiation is contained inside the smallest field of view θ_{min}.

The differential equation for Stokes parameters of doubly scattered radiation can be expressed as:

$$d\mathbf{E}_{rec} = \beta_s^2 \mathbf{R}(\varphi)\left[\mathbf{M}(\pi-\beta)+\theta\cdot\mathbf{M}'(\pi-\beta)\right]\times$$
$$\mathbf{M}(\beta)\mathbf{R}(\varphi)\mathbf{F}_0 \frac{\exp(-2\alpha R)}{R}\Delta s_0 \Delta R \Delta\theta\Delta\varphi d\beta$$

where $\mathbf{F}_0$ and $d\mathbf{E}_{rec}$ are the Stokes vectors for the incident and scattered radiation, β_s and α are the total scattering and extinction coefficients and Δs_0 is the area of the incident beam. The matrix $\mathbf{R}(\varphi)$ rotates the initial coordinate system XYZ around the Z axis at angle -φ, the Mueller matrix $\mathbf{M}$ and its derivative $\mathbf{M}'$ characterize scattering properties of the medium. The scattered power is collected from the volume restricted with angles $\theta+\Delta\theta$, θ, $\varphi+\Delta\varphi$, φ and distances $R+\Delta R$, R. The total received irradiance $\mathbf{E}_{rec}$ is obtained by integration over all possible angles β. Co- and cross-polarized components can be expressed as $\mathbf{E}_{rec,II} = C\mathbf{T}_{II}\mathbf{M}_{eff}(\theta,\varphi,R)\mathbf{F}_0$ and $\mathbf{E}_{rec,\perp} = C\mathbf{T}_{\perp}\mathbf{M}_{eff}(\theta,\varphi,R)\mathbf{F}_0$, where $\mathbf{T}_{II}$ and $\mathbf{T}_{\perp}$ are Mueller matrices for corresponding polarizers, $C=\beta_s^2\Delta s_0\Delta R\Delta\theta\Delta\varphi$, and effective matrix[3,4] $\mathbf{M}_{eff}$ is an integral of the remaining terms in the differential equation. In the case of a medium that is invariant to rotation and reflection (for example, it consists of randomly oriented cylinders, spheroids or spheres), the first elements of the vectors $\mathbf{E}_{rec,II}$ and $\mathbf{E}_{rec,\perp}$ corresponding to detected powers can be expressed as $P_{rec,II} = C(M_{11}+M_{21}+M_{12}+M_{22})/2$ and $P_{rec,\perp} = C(M_{11}-M_{21}+M_{12}-M_{22})/2$, where M_{ij} are elements of the effective matrix. These powers are periodical functions of the angle φ and the minimal period $\pi/2$ will correspond to the case of scattering by spheres.

3. SIMULATION

The irradiance pattern for cross-polarized scattered components is shown in Fig.2. Computations are performed for a cloud base z_a=1000 m, a sounding depth Δz=50m, and a wavelength λ=1.06 μm. Here we introduce the sounding depth as $\Delta z = R_{av} - z_a$, where R_{av} is a projection of w to the axis Z averaged over all possible angles β. Particle size distribution is log-normal with modal radius r_0=10 μm and dispersion lnσ=0.35. Recall that the angle θ in Fig.1 corresponds to one half of lidar FOV. The computed patterns for co- and cross-polarized components are cross shaped and rotated at 45 dg one with respect to the other.

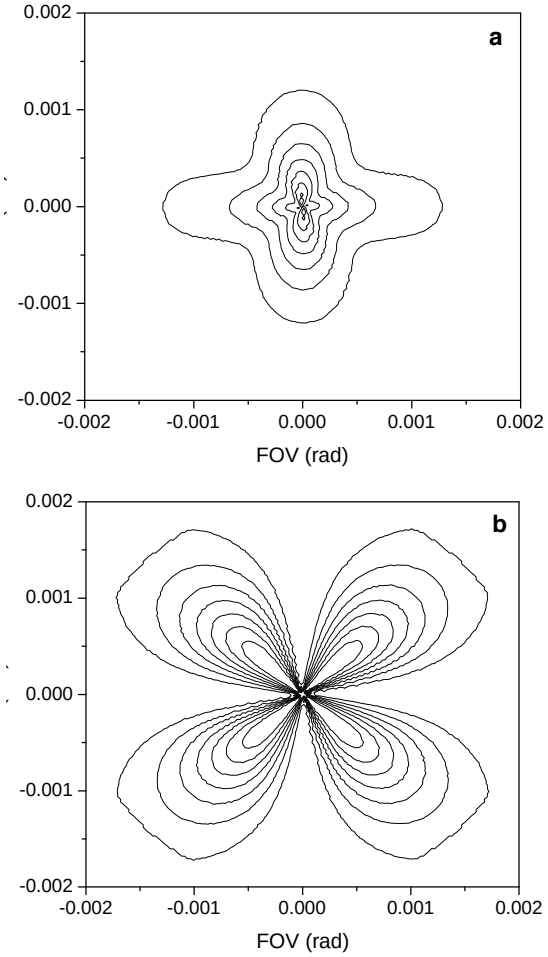

Fig.2. Irradiance patterns for (a) co- and (b) cross-polarized component. Initial polarization is oriented horizontally.

The dependence of the powers of co- and cross-polarized component on angle θ (at φ=0 for $P_{rec,\mathbf{P}}$ and φ=45 dg for $P_{rec,\perp}$) is shown in Fig.3. Calculations are performed for z_a=1000 m and Δz=25, 50, 100 m. The angular distributions $P_{rec,\mathbf{P}}(\theta)$, $P_{rec,\perp}(\theta)$ are determined by the parameter $\eta = \frac{\Delta z}{z_a}$. With the decrease of η the distributions become narrower. For high altitude measurements the scattered intensity is concentrated at

small FOVs thus complicating the lidar design. To alleviate this problem it is desirable to work with long-wavelength radiation, because the width of $P_{rec}(\theta)$ is determined by the ratio $\frac{\lambda}{r}$.

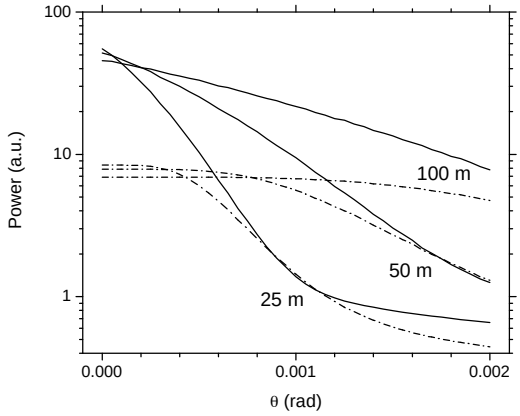

Fig.3. Dependence of powers $P_{rec,\mathbf{P}}$ (solid) and $P_{rec,\perp}(\theta)$ (dash-dot) on FOV. Computations are performed for z_a=1000 m, Δz=25, 50, 100 m; r_0=10 μm.

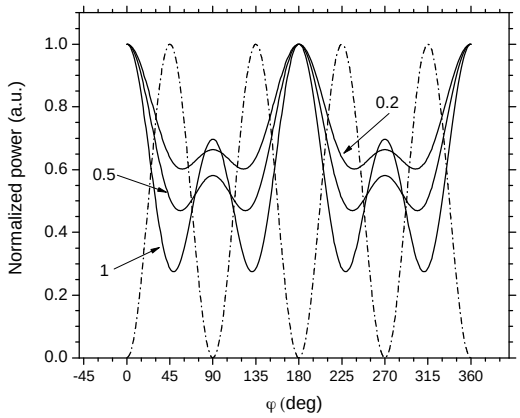

Fig.4. Azimuthal distributions of $P_{rec,\mathbf{P}}$ (solid) and $P_{rec,\perp}$ (dash-dot) for θ= 0.2, 0.5 and 1 mrad. Computations are performed for z_a=1000 m, Δz=50 m, r_0=10 μm.

The azimuthal dependence $P_{rec}(\varphi)$ is a periodical function of φ. Fig.4 shows the azimuthal distributions $P_{rec,\mathbf{P}}(\varphi)$ and $P_{rec,\perp}(\varphi)$ for different values of θ. For convenience of comparison the distributions are normalized to keep the maximal value equal 1. $P_{rec,\perp}(\varphi)$ is proportional to $(1-\cos 4\varphi)$ for all θ. Azimuthal dependence of $P_{rec,\mathbf{P}}$ is more complicated. For small FOV the "modulation depth" is low, i.e. the normalized power doesn't differ much from 1. With the increase of θ the "modulation depth" rises. For all particle size distributions the cross polarized component is cross-shaped and it may be removed if the appropriate mask is inserted in the focal plane of the lidar receiver. The azimuthal rotation of such mask should influence the measured depolarization. Thus it may be used for discrimination of spherical particles from particles of irregular shape even in the presence of multiple scattering.

4. EXPERIMENTAL RESULTS

Lidar measurements reported in the present paper were performed in Potenza (Southern Italy) by the DIFA-Univ. of BASILicata Raman lidar system (*BASIL*). Using Raman/elastic scattering from atmospheric molecules and particles, *BASIL* provides high temporal and spatial resolution measurements of particle backscatter, extinction and depolarization at 355 nm. The lidar system makes use of a tripled Nd:YAG laser source with an average power of 5 W. The receiver is built around a telescope in Newtonian configuration (40 cm diameter). Signal detection is accomplished by means of photomultipliers operated in photon counting mode. The receiver of *BASIL* was opportunely modified for the purposes of this research in order to allow variable-FOV measurements and measurements of the azimuthal dependence of lidar signals.

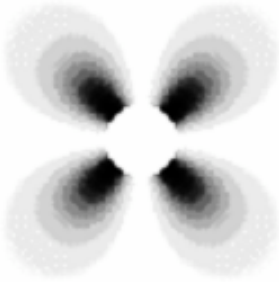

Fig.5. Modeling azimuthal distribution of cross-polarized component for the used lidar parameters.

Since measurements for the different FOVs could not be run simultaneously, we tried to select cloudy conditions characterized by the presence of a stable and uniform cloud deck in order to minimize signal variability associated with variable cloud properties. For the purpose of studying the azimuthal dependence of the polarization pattern a cross-shaped mask was located in the focus of the telescope. This mask has a diameter which corresponds to a FOV of 8.8 mrad, with a circular blocking in the central part of field stop (~ 1.5 mrad) to remove single scattering. The expected

irradiance pattern for these *BASIL* parameters (z_a=400 m, Δz=100 m) is shown in Fig.5. Lidar measurements on 31 January 2006 (16:57-17:12 GMT) with the mask oriented at 0 and 45 deg were performed in sequence (considering an integration time of 5 minute per orientation). Particle depolarization ratio was determined based on the expression:

$$\delta_{par}(z) = \frac{\beta_{par}^{\perp}(z)}{\beta_{par}^{||}(z)} = \frac{R^{\perp}(z)-1}{R^{||}(z)-1}\delta_{mol}(z)$$

where $R^{\perp}(z)$, $R^{\mathbf{P}}(z)$ are the scattering ratios for parallel and perpendicular component, δ_{mol} is taken to be equal to 0.005. Figure 6 shows the depolarization profiles measured with the mask oriented at 0 and 45 deg. The figure clearly highlight the variability of particle depolarization in dependence of mask orientation. Particle depolarization is approximately 50 % larger with the mask at 0 deg (peak depolarization is 0.184) than with the mask at 45 deg (peak depolarization is 0.125). These measurements are not optimized in terms of the operational FOV and mask shape, thus should be considered as preliminary. We expect that after optimization the discrimination between two mask orientations should be much stronger.

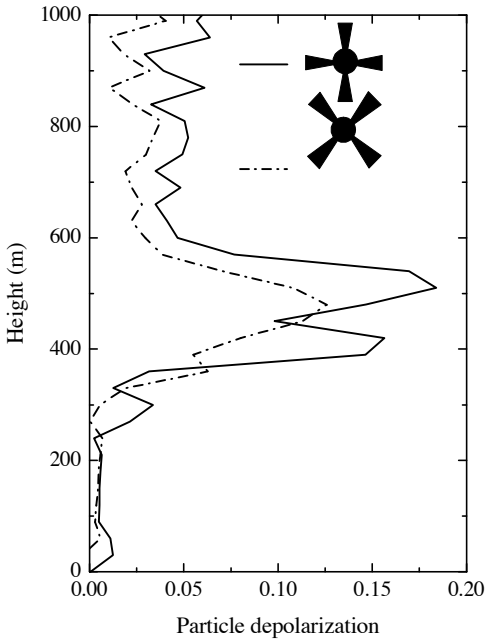

Fig.6. Particle depolarization profiles measured with the cross-shaped mask oriented at 0 and 45 deg.

5. CONCLUSION

We have developed an algorithm for the calculation of intensity distribution of doubly scattered radiation in the focal plane of lidar receiver. The results of lidar measurements confirm that the cross shape patterns of intensity distribution can be used for the discrimination between spherical particles and particles of irregular shape in the presence of strong multiple scattering. Further measurements covering a variety of cloud scenarios will be discussed at the conference. Additional simulations and measurements will be also devoted to the characterization of the radial dependence of the polarization pattern.

REFERENCES

1. Polarization anisotropy in lidar multiple scattering from atmospheric clouds, S. R. Pal and A. I. Carswell, Applied Optics, vol. 24, No. 21, (1 Nov 1985), pp. 3464-3471
2. N. Roy, G. Roy, L. R. Bissonnette and J-R. Simard, 'Measurement of the azimuthal dependence of cross-polarized lidar returns and its relation to optical depth', Appl. Opt. 43, 2777-2785 (2004).
3. M. J. Raković and G. W. Kattawar, "Theoretical analysis of polarization patterns from incoherent backscattering of light", Appl. Opt. 37, 3333-3338 (1998).
4. M. Dogariu, T. Asakura, "Polarization-dependent backscattering patterns from weakly scattering media", J. Optics 24, 271-278 (1993).